Articles

Experimental and Theoretical Study of the Formation of Germanium−Carbon Ion Species in Gaseous Germane/Ethene Mixtures

Paola Antoniotti, Carlo Canepa, Andrea Maranzana, Lorenza Operti,* Roberto Rabezzana, Glauco Tonachini,* and Gian Angelo Vaglio

Dipartimento di Chimica Generale ed Organica Applicata, Università degli Studi di Torino, Corso Massimo d'Azeglio 48, 10125 Torino, Italy

Received June 27, 2000

The gas-phase chemistry of gaseous germane/ethene mixtures has been investigated by ab initio theoretical calculations and by experiments to examine the formation and growth of germanium-/carbon-containing species. Ion/molecule reactions in GeH_4/C_2H_4 mixtures have been studied with an ion trap mass spectrometer. Ion abundance variations as a function of reaction time, reaction paths originating from primary ions of both reagents, and reaction rate constants of the main processes have been determined. The highest yield of new Ge−C bonds formed via reactions of Ge-containing ions with ethene molecules was obtained in mixtures carrying similar amounts of germane and ethene. Reactions of $GeH_2^{\bullet+}$ with ethene play a prominent role in this system. High-level theoretical methods were therefore used to determine the geometrical structures and energies of transition structures, reaction intermediates, and final products for several reaction pathways. Formation of the adduct between $GeH_2^{\bullet+}$ and $H_2C{=}CH_2$ is the initial step. This process is fairly exothermic, and the free energy of the system allows several transformations. Isomerization pathways and H, H_2, or $CH_3^{\bullet}$ loss pathways starting from this adduct have been explored. The free energy threshold defined by the first step shows that some transformations are likely to occur, whereas others can be regarded as inaccessible. Last, two theoretical methods have been used to compute the heats of formation of the attainable $GeC_2H_n^+$ species.

Introduction

The gas-phase ion chemistry of organogermanes is of particular interest on account of their employment in the synthesis of amorphous germanium carbide (a-GeC:H) semiconductors to obtain wide-range light collectors for electronic and optoelectronic devices.[1,2] Laser or X-ray assisted chemical vapor deposition methods[3] are generally applied to prepare a-GeC:H from mixtures of germanium hydride (GeH_4) and small hydrocarbons. Unfortunately, no direct correlation is possible between the germanium and carbon contents of the final solid and the composition of the reacting gaseous system (nature of the hydrocarbon and partial pressures of the reagents). However, since ion species are involved in both the first polymerization steps and the formation of precursors of the solid,[4] their nature and abundance indicate the experimental conditions leading to amorphous solids of the desired composition.

These studies also provide fundamental information on the behavior of selected ion species in the absence of perturbing effects, such as the presence of a solvent or counterions.[5,6] Combined experimental and theoretical investigation in the elucidation of gas-phase ion reaction mechanisms has the advantage of providing complementary information.[6−12] Mass spectrometry is used to describe the overall reactivity of gaseous systems and determine reaction mechanisms and kinetics of isolated

* To whom correspondence should be addressed. Fax: *39 011 670 7591. E-mails: operti@ch.unito.it; tonachini@ch.unito.it.

(1) Ekerdt, J. G.; Sun, Y.-M.; Szabo, A.; Szulczewski, G. J.; White, J. M. *Chem. Rev.* **1996**, *96*, 1499−1518.

(2) Hess, P. *Electronic Material Chemistry;* Dekker: New York, 1996; pp 127−169.

(3) Hitchman, M. L.; Jensen, K. F. *Chemical Vapor Deposition: Principles and Applications*; Academic Press: London, 1993.

(4) (a) Belluati, R.; Castiglioni, M.; Volpe, P.; Gennaro, M. C. *Polyhedron* **1987**, *6*, 441−446. (b) Benzi, P.; Castiglioni, M.; Volpe, P.; Battezzati, L.; Venturi, M. *Polyhedron* **1988**, *7*, 597−600.

(5) Cacace F. *Pure Appl. Chem.* **1997**, *69*, 227−229.

(6) (a) Schröder, D.; Heineman, C.; Koch, W.; Schwarz, H. *Pure Appl. Chem.* **1997**, *69*, 273−280. (b) Jackson, P.; Diefenbach, M.; Schröder, D.; Schwarz, H. *Eur. J. Inorg. Chem.* **1999**, 1203−1210. (c) Jackson, P.; Srinivas, R.; Blanksby, S. J.; Schröder, D.; Schwarz, H. *Chem. Eur. J.* **2000**, *6*, 1236−1242. (d) Jackson, P.; Diefenbach, M.; Srinivas, R.; Schröder, D.; Schwarz, H. *Angew. Chem., Int. Ed. Engl.* **2000**, *39*, 1445−1447.

(7) (a) Bernardi, F.; Cacace, F.; de Petris, G.; Pepi, F.; Rossi, I.. *J. Phys. Chem. A* **1998**, *102*, 1987−1994. (b) Bernardi, F.; Cacace, F.; de Petris, G.; Pepi, F.; Rossi, I.. *J. Phys. Chem. A* **1998**, *102*, 5831−5836.

(8) (a) Cipollini, R.; Crestoni, M. E.; Fornarini, S. *J. Am. Chem. Soc.* **1997**, *119*, 9499−9503. (b) Chiavarino, B.; Crestoni, M. E.; Di Rienzo, B.; Fornarini, S. *J. Am. Chem. Soc.* **1998**, *120*, 10856−10862.

(9) (a) Wlodek, S.; Fox, A.; Bohme, D. K. *J. Am. Chem. Soc.* **1991**, *113*, 4461−4468. (b) Srinivas, R.; Hrušák, J.; Sülzle, D.; Bohme, D. K.; Schwarz, H. *J. Am. Chem. Soc.* **1992**, *114*, 2802−2806.

(10) (a) Reents, W. D., Jr.; Mandich, M. L. *J. Chem. Phys.* **1992**, *96*, 4429−4439. (b) Raghavachari, K. *J. Chem. Phys.* **1992**, *96*, 4440−4448.

10.1021/om0005553 CCC: $20.00
Publication on Web 01/05/2001

ions, while ab initio calculations explore mechanistic details related to the experimental findings, such as the energetics and the structures of the ion intermediates, transition structures, and products.

Ion/molecule reactions in monogermane[13] and experimental data on bond energies in GeH_4 and ionization potentials of the $GeH_n^{\bullet}$ radical species[14] have already been reported, whereas the gas-phase ion chemistry of organogermanes is relatively unexplored. The latest studies are of $Ge(OR)_4$ (R = alkyl) species[15] and mixtures of germane with small molecules (oxygen, ammonia, hydrocarbons, silicon hydrides, and phosphine).[16]

This paper describes the ionic overall reactivity, reaction mechanisms of the most abundant ions, and reaction rate constants of the main processes determined by the ion trap mass spectrometry of germane/ethene systems. The best experimental conditions for formation of Ge−C-containing ions (mixed ions) of increasing size have been investigated for the deposition of amorphous germanium carbides from radiolytically activated gaseous mixtures. The reaction of $GeH_2^{\bullet+}$ with ethene was the most efficient process and gave cluster ions of increasing size, as $SiH_2^{\bullet+}$ does in silane/ethene mixtures.[12] The pathways of this reaction were therefore investigated in depth by quantum chemical calculations to determine the geometries and energies of transition structures, reaction intermediates, and final products. Last, also the G2 composite method[17] was used to compute the standard molar heats of formation of the attainable $GeC_2H_n^+$ species.

Experimental Section

Materials. Germane was prepared and purified as described in the literature,[4] and ethene was supplied by SIAD SpA at 99.99% stated purity. Each reagent gas was dried with sodium sulfate. The GeH_4/C_2H_4 mixtures were prepared in the cell of the ion trap by connecting the flasks to the gas inlet system. Helium was obtained from SIAD SpA as research gas at an extrahigh purity of 99.9999% and used as such.

Mass Spectrometry. All experiments were performed on a Finnigan ITMS mass spectrometer maintained at 333 K to obtain results comparable with studies of other systems.[12] Ion trap mass spectrometry theory and methods are discussed in previous works.[11,12,16] Samples were admitted to the trap via an inlet system modified to permit the simultaneous introduction of three gases through different lines. Pressures measured with a Bayard Alpert ionization gauge were typically $2.0-10.0 \times 10^{-7}$ Torr for germane and ethene and about 5.0×10^{-4} Torr for helium. A calibration factor accounting for the geometry of the instrument[16e] (distance between the gauge and the cell) and the relative sensitivity of the gauge (1.94 for GeH_4, 1.87 for C_2H_4)[18] was applied to calculate the real pressure in the trap. The lines and manifold of the spectrometer were frequently baked out to prevent side reactions with the water background. The scan modes for ion/molecule reaction experiments used to determine the overall reactivity of germane/ethene mixtures, reaction mechanisms and rate constants for reactions of selected ions, and the corresponding calculations have been previously described in detail.[16] The ion species selectively isolated from germane contained the ^{70}Ge (i.e. Ge^+, GeH^+) or the ^{76}Ge (i.e. GeH_2^+, GeH_3^+) isotope. In kinetic experiments, isolation of the precursor ions was generally obtained by the apex method (superimposition of dc and rf voltages) or by resonance ejection (rf voltages only). The latter method causes a lower ion excitation. The similarity of the rate constants determined by these two methods and the single-exponential decay of the abundance of the reacting species suggest that these ions were thermalized by unreactive collisions with the buffer gas.

Ions were formed with an electron beam at an average energy of 35 eV and 1−20 ms ionization times. For the study of reaction mechanisms or for kinetics determinations, a suitable reaction time was applied to maximize the abundance of ions to be stored prior to their isolation. Reactions with neutral molecules in the trap lasting from 50 ms for calculations of rate constants to 1 s for overall reactivity and acquisition were the successive steps.

Methods of Calculation. Rearrangements and dissociations of the initial $c-H_2GeC_2H_4^{\bullet+}$ adduct were assessed by determining the critical points corresponding to stable and transition structures on the relevant energy hypersurface through unconstrained gradient optimization[19] of the geometrical parameters within the density functional theory (DFT).[20] The DFT approach is based on the hybrid exchange-correlation functional composed of the three terms exchange functional proposed by Becke (B3)[21] and the correlation functional of Lee, Yang, and Parr (LYP).[22] The DFT(B3LYP) calculations were carried out with the polarized split-valence shell 6-311G(d,p) basis set.[23] The geometries optimized at this computational level were characterized as energy minima or first order saddle points (transition structures) by diagonalization of the analitically computed Hessian (vibrational frequencies calculations). In the figures, interatomic distances

(11) (a) Antoniotti, P.; Operti, L.; Rabezzana, R.; Splendore, M.; Tonachini, G.; Vaglio, G. A. *J. Chem. Phys.* **1997**, *107*, 1491−1500. (b) Antoniotti, P.; Operti, L.; Rabezzana, R.; Tonachini, G.; Vaglio, G. A. *J. Chem. Phys.* **1998**, *109*, 10853−10863. (c) Antoniotti, P.; Operti, L.; Rabezzana, R.; Tonachini, G.; Vaglio, G. A. *J. Chem. Phys.* **2000**, *112*, 1814−1822.

(12) Antoniotti, P.; Canepa, C.; Operti, L.; Rabezzana, R.; Tonachini, G.; Vaglio, G. A. *J. Phys. Chem. A* **1999**, *103*, 10945−10954.

(13) (a) Northrop, J. K.; Lampe, F. W. *J. Phys. Chem.* **1973**, *77*, 30−35. (b) Senzer, S. N.; Abernathy, R. N.; Lampe, F. W. *J. Phys. Chem.* **1980**, *84*, 3066−3067. (c) Operti, L.; Splendore, M.; Vaglio, G. A.; Franklin, A. M.; Todd, J. F. J. *Int. J. Mass Spectrom. Ion Processes* **1994**, *136*, 25−33.

(14) Ruscic, B.; Schwarz, M.; Berkowitz, J. *J. Chem. Phys.* **1990**, *92*, 1865−1875.

(15) Xavier, L. A.; Riveros, J. M. *Int. J. Mass Spectrom.* **1998**, *179/180*, 223−230.

(16) (a) Benzi, P.; Operti, L.; Vaglio, G. A.; Volpe, P.; Speranza, M.; Gabrielli, R. *J. Organomet. Chem.* **1988**, *354*, 39−50. (b) Benzi, P.; Operti, L.; Vaglio, G. A.; Volpe, P.; Speranza, M.; Gabrielli, R. *J. Organomet. Chem.* **1989**, *373*, 289−300. (c) Benzi, P.; Operti, L.; Vaglio, G. A.; Volpe, P.; Speranza, M.; Gabrielli, R. *Int. J. Mass Spectrom. Ion Processes* **1990**, *100*, 647−663. (d) Operti, L.; Splendore, M.; Vaglio, G. A.; Volpe, P. *Organometallics* **1993**, *12*, 4516−4522. (e) Benzi, P.; Operti, L.; Rabezzana, R.; Splendore, M.; Volpe, P. *Int. J. Mass Spectrom. Ion Processes* **1996**, *152*, 61−68. (f) Antoniotti, P.; Operti, L.; Rabezzana, R.; Vaglio, G. A. *Int. J. Mass Spectrom.* **1999**, *182/183*, 63−71.

(17) Curtiss, L. A.; Raghavachari, K.; Trucks, G. W.; Pople, J. A. *J. Chem. Phys.* **1991**, *94*, 7221−7230.

(18) Decouzon, M.; Gal, J. F.; Maria, P. C.; Tchinianga, A. S. Personal communication.

(19) (a) Pople, J. A.; Gill, P. M. W.; Johnson, B. G. *Chem. Phys. Lett.* **1992**, *199*, 557−560. (b) Schlegel, H. B. In *Computational Theoretical Organic Chemistry*, Csizsmadia, I. G., Daudel, R., Eds.; Reidel: Dordrecht, The Netherlands, 1981; pp 129−159. (c) Schlegel, H. B. *J. Chem. Phys.* **1982**, *77*, 3676−3681. (d) Schlegel, H. B.; Binkley, J. S.; Pople, J. A. *J. Chem. Phys.* **1984**, *80*, 1976−1981. (e) Schlegel, H. B. *J. Comput. Chem.* **1982**, *3*, 214−218.

(20) (a) Parr, R. G.; Yang, W. *Density Functional Theory of Atoms and Molecules*; Oxford University Press: New York, 1989; Chapter 3. (b) Pople, J. A.; Gill, P. M. W.; Johnson, B. G. *Chem. Phys. Lett.* **1992**, *199*, 557−560.

(21) (a) Becke, A. D. *Phys. Rev. A* **1988**, *38*, 3098−3100. (b) Becke, A. D. *ACS Symp. Ser.* **1989**, *394*, 165. (c) Becke, A. D. *J. Chem. Phys.* **1993**, *98*, 5648−5652.

(22) Lee, C.; Yang, W.; Parr, R. G. *Phys. Rev. B* **1988**, *37*, 785−789.

(23) (a) 6-31G: Hehre, W. J.; Ditchfield, R.; Pople, J. A. *J. Chem. Phys.* **1972**, *56*, 2257−2261. (b) 6-31G(d): Hariharan, P. C.; Pople, J. A. *Theor. Chim. Acta* **1973**, *28*, 213−222. (c) 6-311G(d, p): Frisch, M. J.; Pople, J. A.; Binkley, J. S. *J. Chem. Phys.* **1984**, *80*, 3265−3269. The basis set for germanium corresponding to the "6-311G" GAUSSIAN keyword is actually a (15s11p6d) contracted to [8s7p3d], without any sharing of the exponential coefficients.

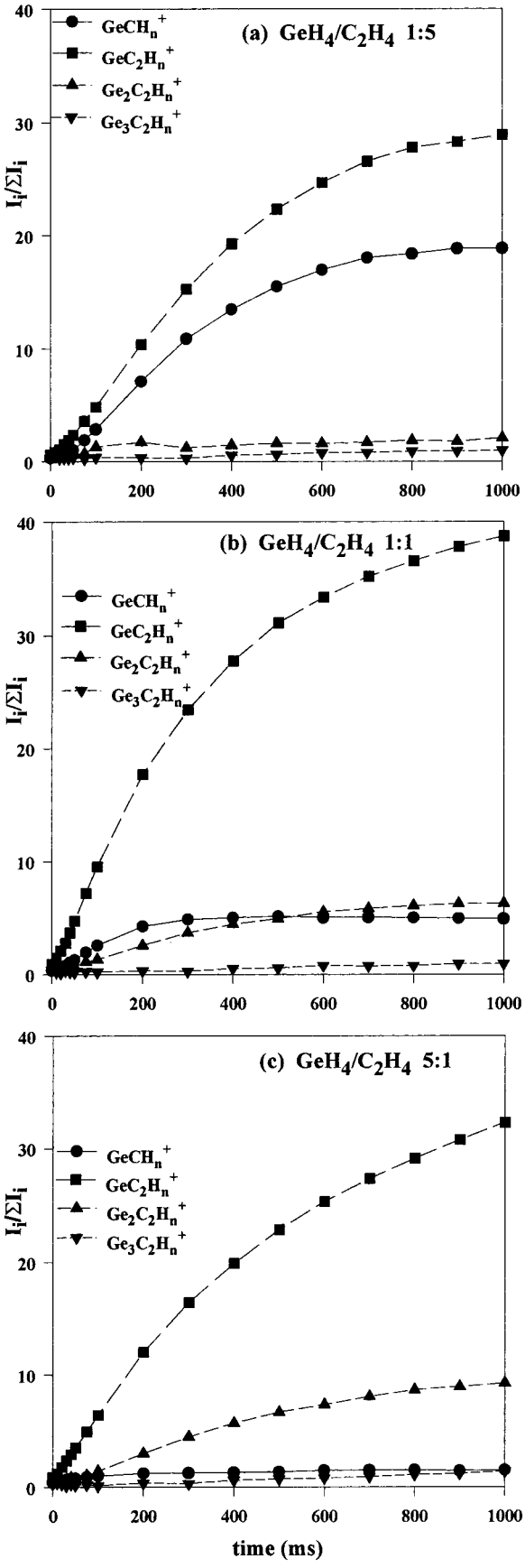

Figure 1. Variation of the abundances with reaction time of the $GeCH_n^+$, $GeC_2H_n^+$, $Ge_2C_2H_n^+$, and $Ge_3C_2H_n^+$ ion families for germane/ethene mixtures in the approximate ratios 1:5 (a), 1:1 (b), and 5:1 (c).

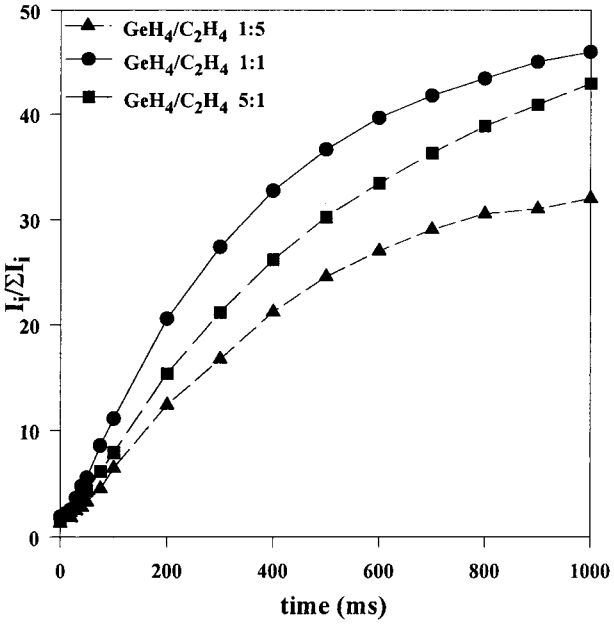

Figure 2. Variation of the sum of the abundances of mixed ions, excluding $GeCH_n^+$, as a function of reaction time for each of the 1:5, 1:1, and 5:1 germane/ethene mixtures.

Scheme 1

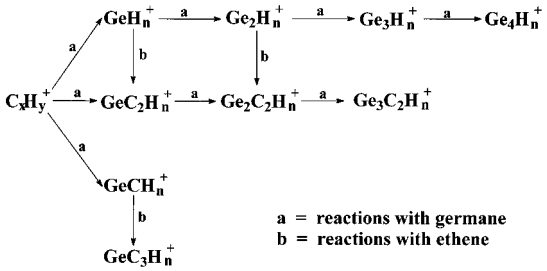

are reported in ångströms and angles in degrees (Mulliken group charges in parentheses and spin densities between square brackets). Standard molar formation enthalpies of the intermediate ions were estimated by DFT theory and the composite procedure G2.[17] The GAUSSIAN98 suite of programs[24−26] was used throughout.

Results and Discussion

Mass Spectrometry. Our initial experiments investigated the formation of germanium- and carbon-containing mixed ions of increasing size as a function of the composition of the reacting mixtures. Three germane/ethene mixtures were examined at a same total pressure of about (1.3−1.4) × 10^{-6} Torr but

(24) Frisch, M. J.; Trucks, G. W.; Schlegel, H. B.; Scuseria, G. E.; Robb, M. A.; Cheeseman, J. R.; Zakrzewski, V. G.; Montgomery, J. A., Jr.; Stratmann, R. E.; Burant, J. C.; Dapprich, S.; Millam, J. M.; Daniels, A. D.; Kudin, K. N.; Strain, M. C.; Farkas, O.; Tomasi, J.; Barone, V.; Cossi, M.; Cammi, R.; Mennucci, B.; Pomelli, C.; Adamo, C.; Clifford, S.; Ochterski, J.; Petersson, G. A.; Ayala, P. Y.; Cui, Q.; Morokuma, K.; Malick, D. K.; Rabuck, A. D.; Raghavachari, K.; Foresman, J. B.; Cioslowski, J.; Ortiz, J. V.; Stefanov, B. B.; Liu, G.; Liashenko, A.; Piskorz, P.; Komaromi, I.; Gomperts, R.; Martin, R. L.; Fox, D. J.; Keith, T.; Al-Laham, M. A.; Peng, C. Y.; Nanayakkara, A.; Gonzalez, C.; Challacombe, M.; Gill, P. M. W.; Johnson, B.; Chen, W.; Wong, M. W.; Andres, J. L.; Gonzalez, C.; Head-Gordon, M.; Replogle, E. S.; Pople, J. A. *Gaussian 98*, Revision A.6; Gaussian, Inc.: Pittsburgh, PA, 1998.
(25) Lippincot, E. R.; Stutman, J. M. *J. Phys. Chem.* **1964**, *68*, 2926−2940.
(26) Kirovac, S.; Bose, T. K. *J. Chem. Phys.* **1976**, *64*, 1580−1582.

Table 1. Rate Constants for Reactions of $C_nH_m^+$ Ions with Germane in Germane/Ethene Mixtures[a]

Ions	product ions (rate constants (k_{exp}))	Σk_{exp}	$k_{collisional}$[b]	Efficiency[c]
C_2H^+	Ge^+ (3.8), GeH^+ (2.0), GeH_2^+ (2.0), GeH_3^+ (0.2)	8.0	12.01	0.67
$C_2H_2^+$	Ge^+ (2.3), GeH^+ (0.9), GeH_2^+ (1.9), GeH_3^+ (2.0)	7.1	11.83	0.60
$C_2H_3^+$	GeH_3^+ (4.4), $GeC_2H_5^+$ (1.2)	5.6	11.66	0.48
$C_2H_4^+$	Ge^+ (1.1), GeH_2^+ (3.9), GeH_3^+ (0.6)	5.6	11.51	0.49
$C_2H_5^+$	GeH_3^+ (3.6)	3.6	11.36	0.32
$C_3H_5^+$	GeH_3^+ (0.9), $GeCH_5^+$ (4.0)	4.9	10.08	0.49

[a] Rate constants are expressed as 10^{-10} cm^3 molecule^{-1} s^{-1}; uncertainty is within 20%. [b]Collisional rate constants have been calculated according to the Langevin theory taking the polarizability of germane (4.966×10^{-24} cm^3) from ref 25 and that of ethene (4.252×10^{-24} cm^3) from ref 26. [c] Efficiency has been calculated as the ratio $k_{exp}/k_{collisional}$.

Table 2. Rate Constants for Reactions of GeH_n^+, $GeC_2H_4^+$, and $Ge_2H_{2-3}^+$ Ions with Germane and Ethene in Germane/Ethene Mixtures[a]

reactants	product ions (rate constants (k_{exp}))	Σk_{exp}	$k_{collisional}$[b]	efficiency[c]
$Ge^+ + GeH_4$	$Ge_2H_2^+$ (6.4)	6.4	8.541	0.75
$GeH^+ + GeH_4$	$Ge_2H_3^+$ (6.0)	6.0	8.511	0.70
$GeH_2^+ + GeH_4$	GeH_3^+ (2.8), $Ge_2H_2^+$ (3.6), $Ge_2H_4^+$ (2.5)	8.9	8.482	1.05
$GeH_2 + C_2H_4$	$GeC_2H_4^+$ (0.8)	0.8	10.69	0.075
$GeH_3^+ + C_2H_4$	$GeC_2H_5^+$ (1.5)	1.5	10.67	0.14
$GeC_2H_4^+ + GeH_4$	$Ge_2C_2H_6^+$ (2.5)	2.5	7.906	0.32
$Ge_2H_{2-3}^+ + C_2H_4$	$Ge_2C_2H_{6-7}^+$ (0.7)	0.7	9.940 9.935	

[a] Rate constants are expressed as 10^{-10} cm^3 molecule^{-1} s^{-1}; uncertainty is within 20%. [b]Collisional rate constants have been calculated according to the Langevin theory taking the polarizability of germane (4.966×10^{-24} cm^3) from ref 25 and that of ethene (4.252×10^{-24} cm^3) from ref 26. [c] Efficiency has been calculated as the ratio $k_{exp}/k_{collisional}$.

containing different relative amounts of the two reagent gases, without isolation of ions and with reaction times up to 1 s. The results were compared to find the most suitable mixture, and this was then used to determine the reaction mechanisms starting from primary ions of both reagents (isolation of selected ions and reaction delays up to 500 ms) and to measure the rate constants of the most interesting processes (isolation of selected ions and reaction times of 50 ms by 0.2 ms steps).

Parts a−c of Figure 1 illustrate the variation of abundances of mixed ions for three germane/ethene mixtures in the approximate ratios 1:5 [$p(GeH_4) = 2.2 \times 10^{-7}$ Torr, $p(C_2H_4) = 11.1 \times 10^{-7}$ Torr], 1:1 [$p(GeH_4) = 6.9 \times 10^{-7}$ Torr, $p(C_2H_4) = 6.7 \times 10^{-7}$ Torr], and 5:1 [$p(GeH_4) = 11.5 \times 10^{-7}$ Torr, $p(C_2H_4) = 2.7 \times 10^{-7}$ Torr], respectively. The remaining ions are primary ions of both reagents ($C_2H_n^+$, $n = 1-4$; GeH_n^+, $n = 0-3$) and secondary ions formed in self-condensation ($C_xH_y^+$ $x = 2-4$, $y = 3, 5, 7$; $Ge_2H_n^+$, $n = 2-4$). The $GeC_2H_n^+$ ions ($n = 3-7$) are always the most abundant and reach almost 40% in the 1:1 system. In the presence of excess ethene, the $GeCH_n^+$ ($n = 3, 5$) ion family displays a marked abundance compared with 5% in the other mixtures. The heaviest condensation products, $Ge_2C_2H_n^+$ ($n = 6, 7$) and $Ge_3C_2H_n^+$ ($n = 10,11$), only show appreciable abundances in the presence of excess germane. These findings agree with those of the second set of experiments in which ion species were isolated and stored to investigate their reaction pathways (Scheme 1).

The $GeCH_n^+$ ($n = 3, 5$) species, abundant in the 1:5 GeH_4/C_2H_4 mixture, are, in fact, given only by secondary hydrocarbon ions $C_3H_5^+$, $C_4H_5^+$, and $C_4H_7^+$, whose formation has a higher yield in the presence of excess ethene. In addition, $GeCH_3^+$ and $GeCH_5^+$ react further very slowly, and their contribution to the growth of the mixed ions is negligible. By contrast, clusterization proceeds through $GeC_2H_n^+$ and $Ge_2H_n^+$ ion species formed in higher abundance in the presence of similar amounts of the reagents or an excess of germane. The highest yield of mixed ions should thus be given by the 1:1 GeH_4/C_2H_4 mixture. This is illustrated in Figure 2, where variations of the sum of the abundances of all the mixed ions, except the unreactive $GeCH_3^+$ and $GeCH_5^+$, are shown as a function of the reaction time for the three mixtures.

Scheme 2

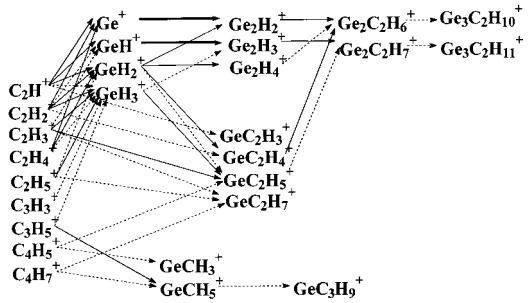

The rate constants of the main reactions leading to Ge-containing ions have also been determined (Tables 1 and 2) to quantify their contribution to the growth of mixed ion species. The collisional rate constants calculated according to Langevin's theory and the reaction efficiencies are also shown in these tables.

Rate constants of self-condensation processes of primary ions of germane, GeH_n^+ ($n = 0-3$), have been already published,[16] and a good agreement is generally observed. Reactions of hydrocarbon ions with germane show good efficiencies, though few products contain both germanium and carbon atoms. By contrast, only GeH_2^+ and GeH_3^+ primary ions react with ethene molecules and display low reaction efficiencies.

Since the $Ge_2H_2^+$ and $Ge_2H_3^+$ secondary ions of germane could not be isolated separately in the rate constant experiments, the value shown in Table 2 was obtained by measuring the rate of disappearance of the whole multiplet and cannot be directly compared with the corresponding collisional rate constants. These results are also summarized in Scheme 2, where thick arrows indicate processes with rate constants higher

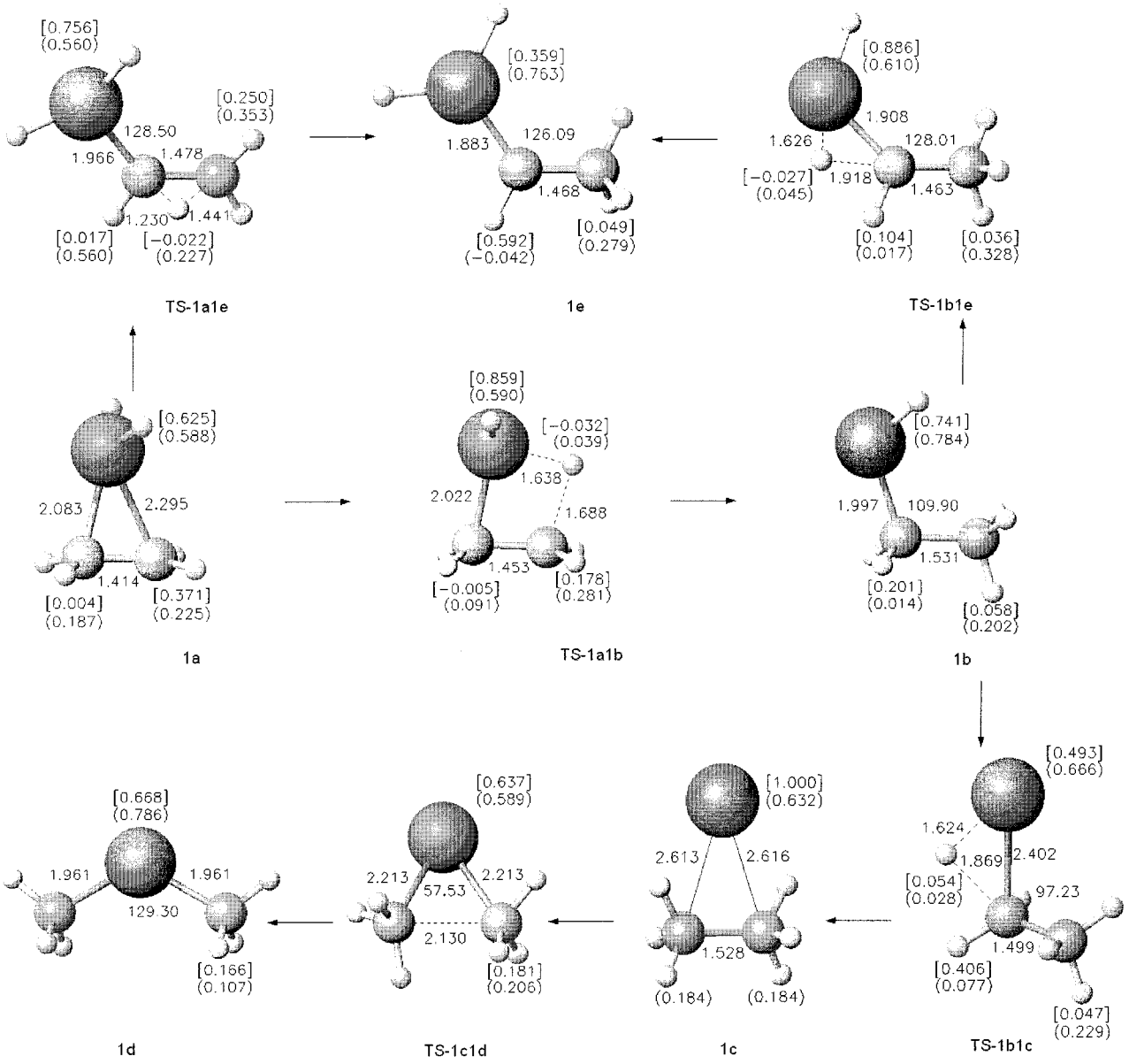

Figure 3. Structures of the $GeC_2H_6^{\bullet+}$ isomers 1a−d, connected by the relevant transition structures (TS). Mulliken group charges (in parentheses) and spin densities (between brackets) are relevant to the GeH_n or CH_n groups.

than 5×10^{-10} cm^3 molecule^{-1} s^{-1}, thin arrows those between 1 and 5×10^{-10} cm^3 molecule^{-1} s^{-1}, and dashed arrows those lower than 1×10^{-10} cm^3 molecule^{-1} s^{-1}, including very slow reactions whose constants could not be determined.

It is evident that the fastest processes, which lead to cluster ions of increasing size, proceed through ions containing two germanium atoms reacting with ethene to form the $Ge_2C_2H_n^+$ ($n = 6, 7$) species. These ions are also given in slower processes from $GeC_2H_n^+$ ($n = 4, 5$) and germane. In both cases, GeH_2^+ is the primary ion that makes the greatest contribution to the formation of the intermediate species. Its reaction pathways were therefore investigated in greater depth by means of ab initio theoretical methods. A similar study has already been published on SiH_2^+ reactions with ethene,[12] to give $SiCH_3^+$, $SiC_2H_4^+$, and $SiC_2H_5^+$ ions. The corresponding Ge-containing ions ($GeCH_3^+$, $GeC_2H_4^+$, and $GeC_2H_5^+$) are thus considered, even though $GeCH_3^+$ has not been experimentally observed.

Theoretical Study of the Reactions. Several processes, possible in principle, were examined. The free energy initially acquired by the system in the formation of the first adduct is available for subsequent isomerizations and fragmentations. Processes estimated to require a larger free energy are not likely to occur. The reactions discussed in the following subsections involve the stable species and the transition structures connecting them, $GeC_2H_6^{\bullet+}$ doublet isomers (Figure 3); $GeC_2H_5^+$ and $GeCH_3^+$ singlet isomers (Figure 5); $GeC_2H_4^{\bullet+}$ doublet isomers (Figure 6). The corresponding energetics are shown in Tables 3−5. The stable structures are sketched with the same labels in the reaction free energy profiles of Figures 4 and 7. Figure 4 shows the profiles that connect the initial adduct c−H_2GeCH_2-$CH_2^{\bullet+}$ (**1a**) to either its isomers or the closed shell fragmentation products obtained by hydrogen atom or methyl radical loss. The isomers of **1a** that result from H shifts and ring opening are numbered as structures **1b**−**e**. The fragments which originate from them by H

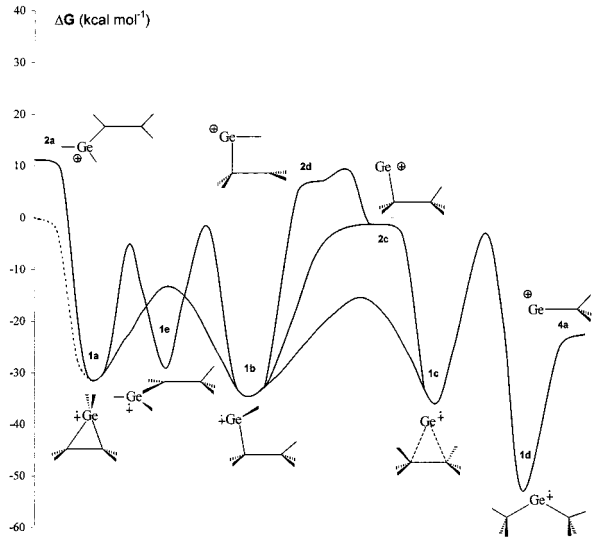

Figure 4. Free energy profiles connecting the $GeC_2H_6^{\bullet+}$ doublet isomers **1a**−**e**. Homolytic cleavage of a C−H bond produces the isomers $GeC_2H_5^+$ **2a**−**d**. Homolytic fragmentation in **1d** can give $GeCH_3^+$ and a methyl radical. The dashed curve connects the two separated reagents to the first adduct, and the horizontal dotted line is the reference free energy corresponding to $GeH_2^{\bullet+}$ and C_2H_4.

loss are numbered as **2a**−**d**. These are the isomeric closed shell ions $GeC_2H_5^+$, which are connected through H shifts. The isomer **2b** does not appear because of its high energy (Table 3). $CH_3^\bullet$ loss from **1d** generates $GeCH_3^+$ (**4a**). Different H_2 losses from the isomers $GeC_2H_6^{\bullet+}$ are represented in Figure 7, where the radical ions of general formula $GeC_2H_4^{\bullet+}$ (**3a**−**d**) are also shown. Further isomerizations through H shifts can, in fact, connect these intermediates (**3a**−**3b**; **3b**−**3c** and **3d**) in principle.

1. Formation of Doublet $GeH_2C_2H_4^{\bullet+}$. The cyclic intermediate **1a** (Figure 3, middle left) forms from the addition of $GeH_2^{\bullet+}$ and $H_2C{=}CH_2$, with a free energy gain of ca. 31 kcal mol^{-1}, at a temperature of 333 K. At variance with the silicon analogue,[12] GeH_2^+ does not interact symmetrically with the two C atoms. The two 2.08 and 2.30 Å Ge−C bonds have essentially the nature of a weakened single Ge−C bond, which is 1.969 Å long in neutral methylgermane, for example, at the same theory level. Furthermore, the C−C bond is significantly elongated to 1.41 Å from its initial value of 1.33 Å in ethene. This indicates that the π system is partially disrupted by a substantial electron donation into the originally empty orbital of the $GeH_2^{\bullet+}$ radical cation. The positive charge of the cyclic radical ion is delocalized on the whole structure, as shown by the Mulliken group charges Q (shown between parentheses in Figure 3). By contrast, the unpaired electron is more localized on the GeH_2 group and only one CH_2 group. This is suggested by the excess α electron density, P^α, over the β, P^β (spin density, ΔP) reported between brackets for each XH_n group in Figure 3. In the case of silicon,[12] the symmetric geometry was reflected in spin densities equally shared between the two carbons. The total spin eigenvalue $\langle S^2 \rangle$ is close to 0.75 (Table 3), and contamination by higher spin multiplicities is not large.

2. Isomerization via H Atom Migration and C−Ge or C−C Bond Cleavage. The structural relationships between the initial intermediate **1a** and its isomers are shown in Figure 3, and the relevant energetics are reported in Table 3. Intermediate **1a** can directly transform into its isomers **1b** and **1e** by different hydrogen shifts that involve ring opening. These two migrations require the overcoming of energy barriers

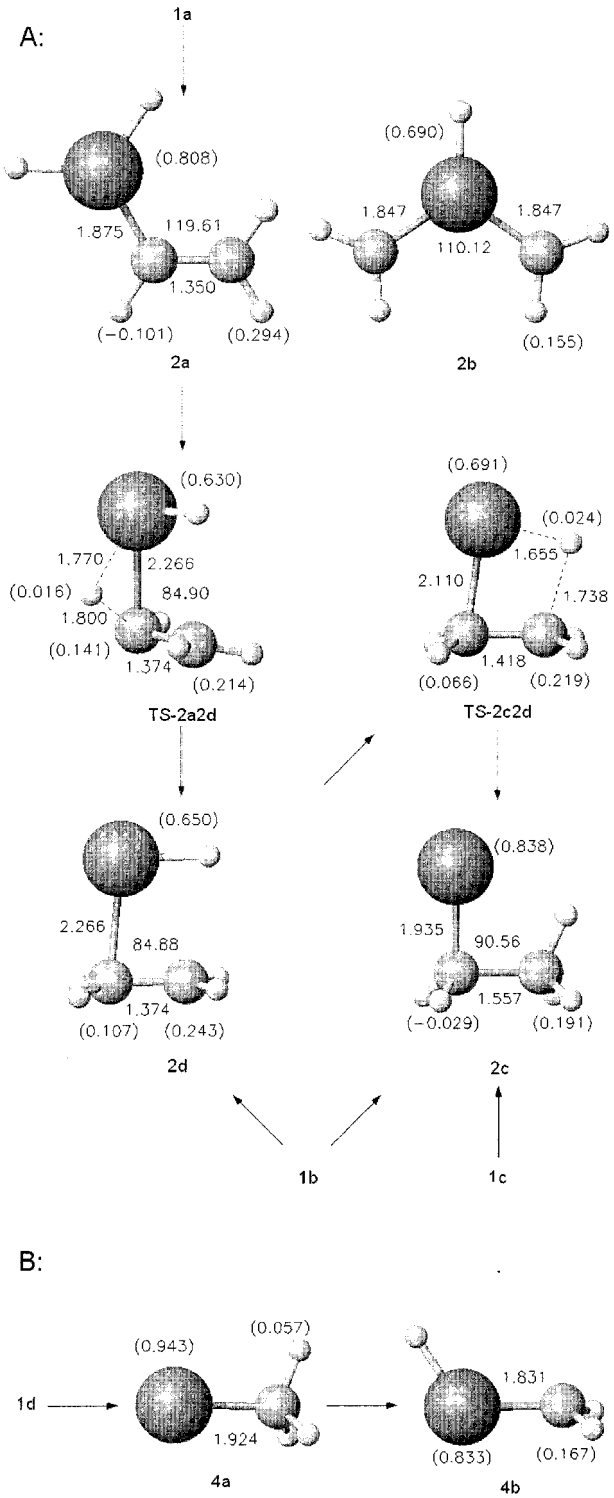

Figure 5. (A) Structures of the $GeC_2H_5^+$ singlet isomers **2a**−**d**, produced from isomers **1** by H loss. Isomers **2c** and **2d** are connected by a H-shift transition structure (TS). Mulliken group charges (in parentheses) are relevant to the GeH_n or CH_n groups. (B) singlet $GeCH_3^+$, **4a**, produced from **1d** by detachment of a methyl radical, and its isomer **4b**.

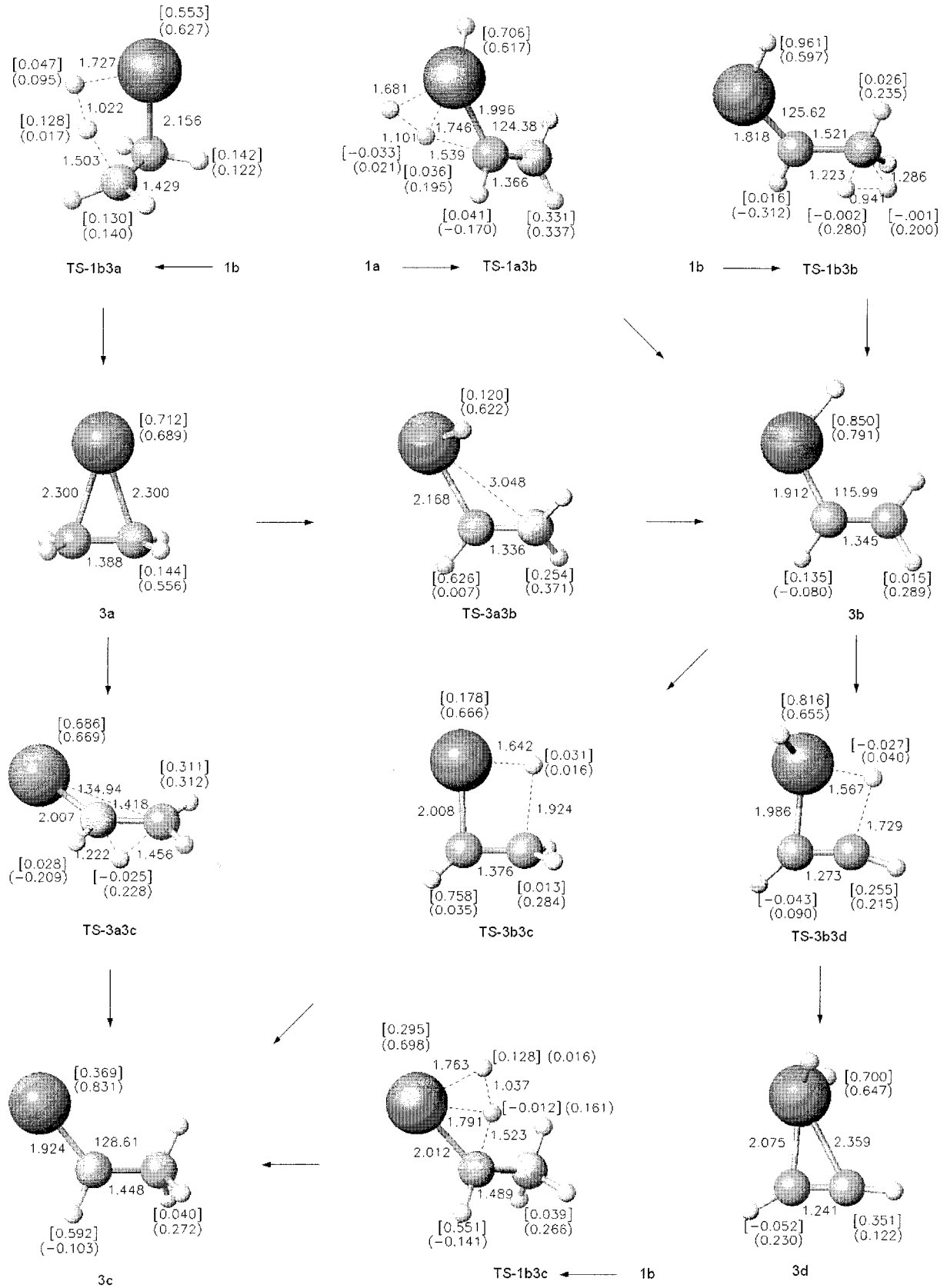

Figure 6. Structures of the $GeC_2H_4^{\bullet+}$ isomers **3a**−**d**, produced from isomers **1** by H_2 loss. Isomers **3** are connected by H-shift transition structures (TS). Mulliken group charges (in parentheses) and spin densities (between brackets) are relevant to the GeH_n or CH_n groups.

that are 13 and 5 kcal mol^{-1} below the threshold defined by the free energy initially acquired by the system (Figure 4).

The energy minimum of **1b** is slightly deeper than that of **1a** (ca. −34 kcal mol^{-1} with respect to the $GeH_2^{\bullet+}$ + $H_2C{=}CH_2$ dissociation limit). Isomer **1e** is only slightly less stable than **1a** (ca. 30 kcal mol^{-1} below the same limit). Isomer **1b** can transform into **1c** through

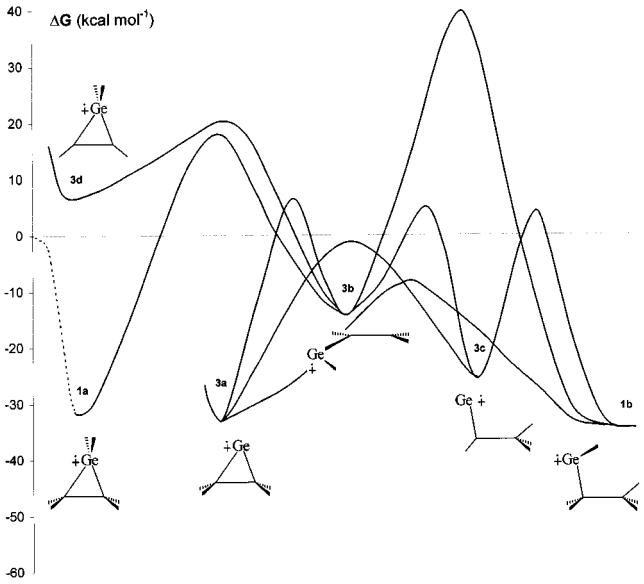

Figure 7. Free energy profiles connecting the $GeC_2H_4^{\bullet+}$ doublet isomers **3a**−**d**. H_2 loss from **1a** and **1b** produces isomers **3**. The dashed curve connects the two separated reagents to the first adduct, and the horizontal dotted line is the reference free energy corresponding to $GeH_2^{\bullet+}$ and C_2H_4.

Table 3. Relative Energies, Enthalpies, and Free Energies (kcal mol^{-1})[a] of the Isomers of $GeC_2H_6^{\bullet+}$ and $GeC_2H_5^+$ (and $GeCH_3^+$) and the Relevant Transition Structures[b]

species	ΔE	ΔZPE	$\langle S^2\rangle$	ΔH^{333}	ΔG^{333}
$GeH_2^{\bullet+} + C_2H_4$	0.0	0.00	0.7523	0.0	0.0
1a	−44.9	3.24	0.7553	−42.7	−31.4
1b	−48.8	4.74	0.7530	−44.9	−34.4
1c	−55.3	7.36	0.7526	−49.1	−38.0
1d	−66.4	5.21	0.7522	−61.6	−53.0
1e	−42.0	2.87	0.7528	−40.1	−28.9
2a	10.9	−3.16	0.0000	8.0	11.2
2b	54.9	−3.47	0.0000	52.0	54.8
2c	−5.2	0.19	0.0000	−4.8	−1.7
2d	5.3	−1.51	0.0000	4.1	7.2
4a	−22.1	0.73	0.0000	−20.9	−22.5
4b	30.3	−2.09	0.0000	28.9	26.9
TS-**1a1b**	−27.2	2.86	0.7550	−26.0	−13.3
TS-**1a1e**	−16.1	0.76	0.7551	−16.5	−5.0
TS-**1b1c**	−28.3	3.40	0.7563	−25.8	−15.4
TS-**1b1e**	−13.5	1.46	0.7546	−13.3	−1.6
TS-**1c1d**	−18.2	4.90	0.7523	−14.4	−3.1
TS-**2a2d**	47.3	−4.76	0.0000	*c*	*c*
TS-**2c2d**	7.4	−1.86	0.0000	5.2	9.5

[a] DFT(B3LYP)/6-311G(d,p) theory level. [b] *H* and *G* of the hydrogen atom or methyl radical taken into account when appropriate. [c] Not computed because of its very high energy.

a viable H-shift pathway (the barrier is −15 kcal mol^{-1} relative to the threshold defined above). The stability of **1c** is greater than that of the preceding isomers (ca. 38 kcal mol^{-1} below the dissociation limit). Two further isomerizations, one connecting **1b** and **1e** (Figure 3, top right), the other connecting **1c** and **1d** (Figure 3, bottom), show energy barriers closer to the same threshold (−2 and −3 kcal mol^{-1}, respectively). The latter is a different process that requires the cleavage of the C−C bond concerted with the formation of two Ge−C bonds. In **1c**, this cleavage requires a significant amount of energy. Even so, it is not sheer, but also causes germanium to become bound to both methyl carbons in yielding isomer **1d**. This open-chain structure

Table 4. Relative Energies, Enthalpies, and Free Energies (kcal mol^{-1})[a] of the Isomers of $GeC_2H_6^{\bullet+}$ and $GeC_2H_4^{\bullet+}$ and the Relevant Transition Structures[b]

species	ΔE	ΔZPE	$\langle S^2\rangle$	ΔH^{333}	ΔG^{333}
$GeH_2^{\bullet+} + C_2H_4$	0.0	0.00	0.7523	0.0	0.0
3a	−36.3	0.08	0.7519	−35.7	−33.7
3b	−13.0	−2.76	0.7530	−14.9	−13.2
3c	−26.9	−0.94	0.7528	−27.2	−25.6
3d	12.0	−6.55	0.7555	6.9	7.1
TS-**1a3b**	7.8	−0.57	0.7671	6.0	17.8
TS-**1b3a**	−21.4	2.01	0.7538	−21.0	−8.6
TS-**1b3b**	28.2	1.22	0.7561	28.3	39.8
TS-**1b3c**	−7.1	1.19	0.7600	−7.3	4.4
TS-**3a3b**	9.1	−5.06	0.7571	5.2	6.4
TS-**3a3c**	−1.2	−2.75	0.7565	−3.4	−1.2
TS-**3b3c**	6.7	−4.75	0.7603	2.4	4.8
TS-**3b3d**	24.0	−6.62	0.7589	17.9	20.3

[a] DFT(B3LYP)/6-311G(d,p) theory level. [b] *H* and *G* of the hydrogen molecule taken into account when appropriate.

Table 5. Standard Molar Formation Enthalpies (kcal mol^{-1}) at the DFT(B3LYP)/6-311G(d,p) and G2 Results for the Isomers $GeC_2H_6^{\bullet+}$, $GeC_2H_5^+$, $GeC_2H_4^{\bullet+}$, and $GeCH_3^+$

	ΔH_f° (298K)			ΔH_f° (298K)	
species	DFT	G2	species	DFT	G2
1a	241.1	238.7	**2c**	226.6	223.4
1b	238.9	238.8	**2d**	235.4	234.1
1c	234.8	234.7	**3a**	248.0	249.1
1d	222.1	220.6	**3b**	268.7	269.0
1e	243.7	244.5	**3c**	256.6	260.1
2a	239.4	235.7	**3d**	290.4	286.2
2b	283.3	275.7	**4a**	227.8	226.7

resembles that of $:Ge(CH_3)_2$, but with one electron less, and is the most stable $GeC_2H_6^{\bullet+}$ isomer, since it is located 54 kcal mol^{-1} below the $GeH_2^{\bullet+} + H_2C{=}CH_2$ dissociation limit. The two sequential isomerizations from **1a** to **1b** and from **1b** to **1c** are thus the easiest transformations. A similar picture was obtained for silicon.[12] All the silicon analogues of **1** were to some extent more stable with respect to the dissociation limit, with the exception of that of the silicon analogue of **1c**, namely, the complex of Si^+ with ethane (see below).

Further details emerge from Figure 3, where the structural information is accompanied by data on the electron distribution in the isomers. In the hydrogen migration **1a**−**1b**, formation of a terminal methyl group both elongates the C−C bond and tightens the Ge−C bond. In **1b**, both the electric charge and the unpaired electron are concentrated on the GeH group (Q_{GeH} = 0.78 e and ΔP_{GeH} = 0.74). Starting from **1b**, a further hydrogen shift from germanium to the adjacent carbon has been shown to produce **1c**, a complex in which ethane has formed. The radical cation $Ge^{\bullet+}$ remains loosely associated with this ethane, as shown by the Ge−C distances, larger than 2.61 Å. The spin density ascribes the unpaired electron to germanium entirely (in contrast with the silicon result[12]), whereas the electric charge is to some extent delocalized (0.37 e on ethane, the rest on germanium). Then, the concerted transformation of **1c** into **1d** generates a structure in which the Ge−C bond lengths are close to that of methylgermane. As in **1b**, both the electric charge and the unpaired electron are rather concentrated on the germanium atom (Q_{GeH} = 0.79 e and ΔP_{GeH} = 0.67). Last, isomer **1e** (obtainable from either **1a** or **1b**) has a

rather short Ge−C bond, which indicates some double bond character (the Ge−C bond is 1.778 Å long in H_2GeCH_2, at this computational level). The spin density datum indicates that the unpaired electron is associated with this Ge−C bond, as for silicon.[12]

3. Fragmentation of the Isomers $GeC_2H_6^{\bullet+}$. A single hydrogen atom can be homolytically detached from each of the isomeric species **1** to originate different $GeC_2H_5^+$ closed shell species **2**.

The relevant energetics are reported in Table 3. Figure 5A displays the structural information together with the group charges in the isomers. Two H loss processes are estimated to require 11 (that leading to **2a**) and 7 (that leading to **2d**) kcal mol^{-1} more than the amount of free energy available (see Figure 4). Thus, the relevant singlet cations **2a** and **2d** (Figure 5A) are not likely to form, whereas the isomer **2c** is located 2 kcal mol^{-1} below the energy of the reference dissociation limit and could be attainable. In the silicon case,[12] isomer **2a** was estimated to lie just below the $SiH_2^{\bullet+} + C_2H_4$ reference level, **2d** somewhat higher than its Ge analogue, and **2c** slightly above the reference level. The value of the GeCC angle in isomer **2c** is close to 90° and corresponds to a Ge−terminal C distance of 2.5 Å, indicating some interaction of germanium with the methyl group (compare **1c** in Figure 3). It can be seen that the Ge−C bond is slightly shorter than that in methylgermane. The $H_2C-GeH-CH_2^+$ isomer **2b** is reported in Figure 5 (top), but it does not appear in Figure 4 because its energy is too high, as was the case for its silicon analogue.[12] The GeH_n group owns the largest share of positive charge in all the structures in Figure 5A. The highest concentration of charge on Ge is found in **2c**.

Fragmentation of the radical ion **1d** into a methyl radical and the closed shell $GeCH_3^+$ cation is also plausible (Figure 4, right side, and Figure 5B), whereas isomerization of $GeCH_3^+$ to $HGeCH_2^+$ is not feasible (Table 3). Similar results were obtained for silicon.[12]

4. H_2 Dissociations from the $GeC_2H_6^{\bullet+}$ Isomer. H_2 loss from the $GeC_2H_6^{\bullet+}$ isomers **1** could lead to the $GeC_2H_4^{\bullet+}$ species **3** shown in Figure 6. Isomer **3d** is 7 kcal mol^{-1} above the $GeH_2^{\bullet+} + H_2C{=}CH_2$ limit, whereas isomers **3a**−**c** are stable and located at −34, −13, and −26 kcal mol^{-1}, respectively (Table 4, Figure 7).

However, the transition structures for the pathway connecting **1a** to **3b** appear to be located too high in energy. Yet, transformation of **1a** into **1b** could subsequently lead to **3a** by overcoming a barrier below the threshold and possibly to **3b** and **3c** through transition structures lying just above it, which means that some of these processes may be viable.

The transition structure connecting **1b** to **3a** in Figure 6 (TS-**1b3a**, top left) has no silicon counterpart, whereas the TS-**1a3a** found for silicon could not be located.[12] Apart from this qualitative difference, the easiest pathways for the germanium and the similar silicon systems do not always correspond. For instance, the **3b**−**3d** pathway for silicon has a barrier of ca. 9 kcal mol^{-1} above the reference level, and the silicon analogue of **3d** is significantly below the same level, whereas the equivalent germanium structures are higher in energy. Moreover, the **1a**−**3b** pathway for silicon has a barrier only 4 kcal mol^{-1} above the reference level, whereas its **3a**-**3b** and **3a**-**3c** pathways are more difficult than those for the germanium analogues, whose barriers are 12 and 5 kcal mol^{-1} above the reference level, respectively.[12]

5. Thermochemistry. Standard molar formation enthalpies for the cations were calculated with the G2 method and compared with the DFT(B3LYP)/6-311G-(d,p) estimates in Table 5. The difference between the two sets of values does not exceed 2.7% (structure **2b**).

The formation enthalpies relate to four processes:

$$Ge^+(g) + 2C(s) + 3H_2(g) \rightarrow GeC_2H_6^{\bullet+} \quad (1)$$

$$Ge^+(g) + 2C(s) + {}^5/_2H_2(g) \rightarrow GeC_2H_5^+ \quad (2)$$

$$Ge^+(g) + 2C(s) + 2H_2(g) \rightarrow GeC_2H_4^{\bullet+} \quad (3)$$

$$Ge^+(g) + C(s) + {}^3/_2H_2(g) \rightarrow GeCH_3^+ \quad (4)$$

Two experimental values were employed to relate the computed gas-phase enthalpies for C and Ge^+ to the standard states C(s) and Ge(s):[27−28]

$$C(s) \rightarrow C(g)(^3P) \qquad \Delta H_f^\circ(298K) = 171.3 \text{ kcal mol}^{-1} \quad (5)$$

$$Ge(s) \rightarrow Ge^+(g)(^2P) + e \qquad \Delta H_f^\circ(298K) = 272.2 \text{ kcal mol}^{-1} \quad (6)$$

Conclusions

This investigation of the gas-phase ion/molecule reactions in germane/ethene mixtures has illustrated the experimental conditions that promote the formation of mixed ions of increasing size. Mixed aggregates grow more in systems containing similar partial pressures of the reagent gases or excess GeH_4, since the initial, favored steps of the chain propagation involve primary and secondary ions of germane reacting with ethene molecules. Primary GeH_n^+ ($n = 0-3$) ions are also produced from $C_xH_y^+$ species and germane. The Ge−C-containing species in a flow system that eventually lead to amorphous germanium carbides of a desired composition can thus be prepared by varying the relative amounts of the two reagent gases.

The experimental data show that GeH_2^+ plays a major role in the preparation of mixed ions. High-level theoretical methods were therefore used to examine its reactions with ethene.

Hydrogen atom and hydrogen molecule dissociations from the initial adduct produced by the collision of $GeH_2^{\bullet+}$ onto $H_2C{=}CH_2$ and from other intermediates derived from it have been investigated by correlated ab initio methods. The free energy released in formation of the adduct (ca. 31 kcal mol^{-1}) provides a reference value for determining which rearrangement and cleavage intermediate products are attainable. H shifts in the $GeC_2H_6^{\bullet+}$ species connect rather stable isomers via transition structures located below the free energy threshold. Another isomer is attainable via a C−C bond

(27) Lias, S. G.; Bartmess, J. E.; Liebman, J. F.; Holmes, J. L.; Levin, R. D.; Mallard, W. G. *J. Phys. Chem. Ref. Data Suppl.* **1988**, *17*.

(28) *MolMol 2.4*, release 2K.1; A graphic program; Institut für Molekular-biologie und Biophysik, EHT Zurich Spectrospin AG: Faellenden, Switzerland. Koradi, R.; Billeter, M.; Wüthrich, K. *J. Mol. Graphics* **1996**, *14*, 51−55.

cleavage concerted with the formation of two Ge−C bonds. H loss from these radical ions only once affords a $GeC_2H_5^+$ isomer (**2c**). Other $GeC_2H_5^+$ isomers lie above the reference dissociation limit ($GeH_2^{\bullet+} + H_2C{=}CH_2$) by 7 (**2d**) and 11 (**2a**) kcal mol^{-1}. Theoretical calculations indicate that fragmentation of **1d** to $GeCH_3^+$ (**4a**) is feasible. However, formation of $GeCH_3^+$ from GeH_2^+ and ethene was not observed, probably for kinetic reasons on account of the number of isomerizations required from **1a** to **1d**.

H_2 loss from the $GeC_2H_6^{\bullet+}$ isomers could lead to $GeC_2H_4^{\bullet+}$ species **3a**−**c** (located at −13, −26, and −34 kcal mol^{-1}, respectively, from the $GeH_2^{\bullet+} + H_2C{=}CH_2$ limit). However, the relevant transition structures appear to be located too high in energy, apart from one lying only 3 kcal mol^{-1} above the limit.

Last, theoretical calculations of the enthalpies of formation of the $GeC_2H_n^+$ ions with the G2 and the DFT(B3LYP) methods gave very similar results.

Acknowledgment. Financial support was provided in part by the Italian MURST through the "Cofinanziamento di Programmi di Ricerca di Rilevante Interesse Nazionale", within the project "Chimica in Fase Gassosa di Specie Reattive Neutre e Cariche". Figures 3, 5, and 6 were drawn with the MolMol[28] program.

Supporting Information Available: Tables showing G2 energies at 0 K and DFT energies, enthalpies, and free energies. This material is free of charge via the Internet at http://pubs.acs.org.

OM0005553